

Exchange and hyperfine interaction in AuFe alloys around the percolation threshold

N. N. Delyagin, A. L. Erzinkyan, V. P. Parfenova, and S. I. Reyman

*D. V. Skobel'tsin Research Institute for Nuclear Physics, M. V. Lomonosov Moscow State University
119899 Moscow, Russia*

G. M. Gurevich and S. V. Topalov

Institute for Nuclear Research, Russian Academy of Sciences, Moscow, Russia

M. Trhlik

Karlov University, Prague, Czech Republic

(Submitted 11 July 1995)

Zh. Éksp. Teor. Fiz. **109**, 1451–1464 (April 1996)

Au_{1-x}Fe_x magnetic alloys with iron concentration both below and above the percolation threshold ($x=0.14$ and 0.18) have been studied using the Mössbauer spectroscopy in the temperature range of 5–300 K and in an external magnetic field of 0.2 to 4 T. The spectra have been processed taking into account the anisotropy of the hyperfine interaction in atomic configurations with a nonspherical distribution of electron density. Spectra recorded at temperatures above 5 K have been processed using a new model in order to derive distributions of both hyperfine and exchange fields acting on Fe atoms. Some features of the distribution functions indicate that the exchange field is highly nonuniform, which is due to the competition between the strong direct Fe–Fe exchange at a short range and the weaker indefinite indirect long-range exchange. A magnetic phase transition due to the competition between the two types of exchange predicted by Saslow and Parker¹¹ has been detected in AuFe18 in a weak external magnetic field. © 1996 American Institute of Physics. [S1063-7761(96)02804-1]

I. INTRODUCTION

Depending on the iron content and temperature, various modes of magnetic ordering are observed in Au_{1-x}Fe_x. A magnetic phase diagram of the AuFe alloy is given in Fig. 1.¹ For an iron content below the percolation threshold, $x_c \approx 0.155$, a transition from the paramagnetic to spin-glass state takes place at a temperature T_g . At iron concentrations higher than the critical value, ferromagnetic ordering occurs in the system at the Curie temperature T_C . In the range of concentrations $0.155 \leq x \leq 0.24$ a second magnetic transition to the spin-glass state occurs at a temperature $T_f < T_C$. The properties of such alloys, called reentrant spin glasses, have been studied by various techniques (see Refs. 1–8 and references therein).

Several alternative interpretations of the magnetic properties of structures with reentrant spin-glass behavior have been proposed. In the model by Gabay and Toulouse⁹ the two magnetic transitions are ascribed to the freezing of transverse spin components (of longitudinal components in case of ferromagnetic ordering) in a system with an exchange interaction that changes sign. Note that this approach is only legitimate in systems with classical spin vectors. The model proposed by Beck¹⁰ is based on the assumption that there are weakly interacting ferromagnetic clusters. The model of Saslow and Parker¹¹ considers magnetic ordering in a two-dimensional lattice of Heisenberg spins with competing (ferro- and antiferromagnetic) exchange interactions. This model does not include the oscillating exchange interaction typical of spin glasses, but the main conclusions of the model are quite general and can be applied to any system with

competing exchange interactions. The models mentioned above are based on different and sometimes incompatible assumptions. The data which have been available until recently are insufficient to make an unequivocal choice among these concepts.

In our study we have used Mössbauer spectroscopy to obtain new data about the local magnetic behavior of iron atoms in two Au_{1-x}Fe_x alloys with iron concentration below and above the percolation threshold ($x=0.14$ and $x=0.18$). We focused our attention on the temperature dependence of the parameters of the hyperfine interaction and on the spin alignment in both strong and weak magnetic fields. We have analyzed the shapes of Mössbauer absorption spectra using a new model, which allows us to account for the spectral shapes at low temperature and to derive the distribution functions not only of hyperfine magnetic fields acting on Fe atoms, but also of exchange fields at various temperatures.

II. EXPERIMENTAL TECHNIQUES

The alloys AuFe14 and AuFe18 were fabricated by melting in an arc furnace in argon atmosphere. After homogenization, the samples were rolled to foils with a thickness of about 10 μm , annealed at 800 °C and quenched.

Mössbauer absorption spectra of ⁵⁷Fe were measured with an electrodynamic spectrometer operating in a constant acceleration mode with a ⁵⁷Co source in a Cr matrix and an activity of 50 mCi. Gamma radiation with an energy of 14 keV was detected by a NaI(Tl) scintillation detector 0.1 mm thick or a gas-discharge resonant detector. The samples were placed in a gas-flow helium cryostat. The temperature in the

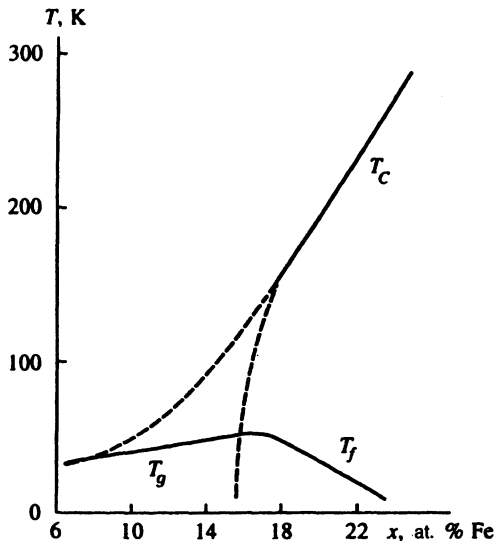


FIG. 1. Magnetic phase diagram of $Au_{1-x}Fe_x$ alloy.¹

experiments was stabilized to within 0.5 K using an electronic circuit. Strong longitudinal magnetic fields of up to 4 T were generated by a superconducting solenoid. A transverse magnetic field of 0.2 T was generated by a permanent magnet. The techniques for processing spectra and calculating distribution functions of hyperfine and exchange magnetic fields will be described in the next section.

III. SPECTRA-ANALYSIS TECHNIQUE AND EXPERIMENTAL RESULTS

3.1. Shapes of spectra at $T=5$ K

A Mössbauer absorption spectrum of the AuFe18 alloy recorded at $T=5$ K is given in the top part of Fig. 2. The

spectrum has a typical asymmetric shape resembling spectra of ^{57}Fe in some intermetallics with two nonequivalent positions of Fe atoms. Previously such spectra were processed using a formal procedure based on an assumption about the existence of two specific states of Fe atoms with two independent distributions of hyperfine fields.^{3,6,7} Investigations of crystalline and magnetic structures of AuFe alloys do not justify this assumption, so this processing technique is apparently incorrect. In quenched AuFe alloys the distribution of Fe atoms is random (or very close to random), hence the spectrum shape at $T=5$ K should be accounted for without any *a priori* statements about the alloy structure. This is necessary for a correct interpretation of the temperature dependence of hyperfine-interaction and exchange-field parameters.

The hyperfine structure of the spectrum at 5 K can be interpreted in terms of a simple model taking into account familiar features of the hyperfine interaction of Fe atoms in metal systems. Mössbauer absorption spectra of AuFe alloys in the paramagnetic state are superpositions of quadrupole doublets due to atomic configurations with different number of Fe atoms in the first coordination sphere.¹² The quadrupole splitting constant in some configurations is as much as 1.4 mm/s. It is obvious that the highly nonspherical distribution of the electron density should lead not only to the quadrupole splitting, but also to a large anisotropic contribution to the magnetic hyperfine field B_{hf} . Below we will see that by analyzing the angular dependence of B_{hf} and quadrupole shift of hyperfine components concurrently we can obtain a self-consistent interpretation of the observed spectrum asymmetry under the condition of a random distribution of Fe atoms in the lattice sites.

The asymmetry of spectra shown in Fig. 2 suggests that there is a permanent correlation between the hyperfine field

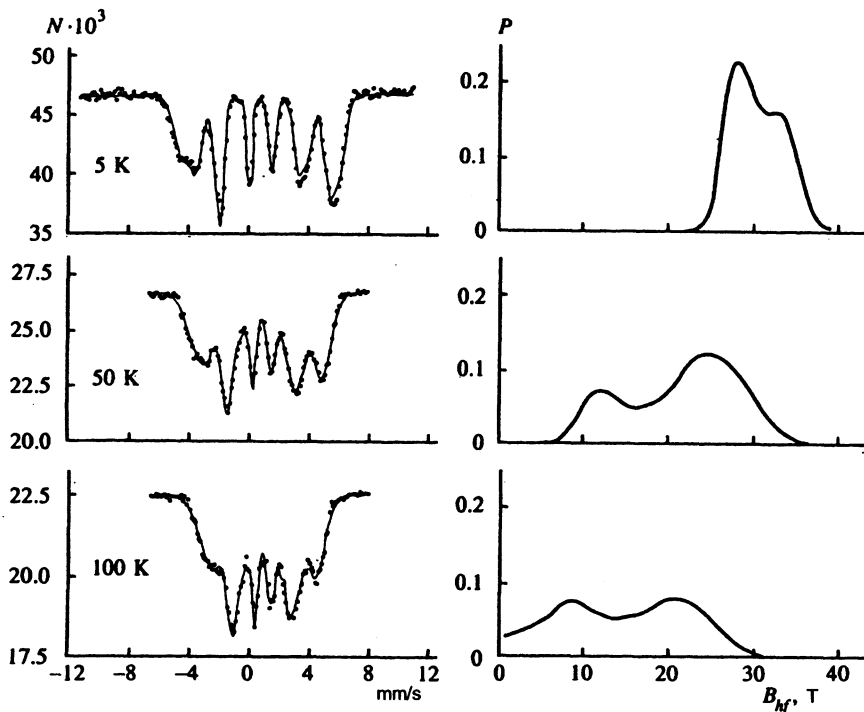


FIG. 2. Mössbauer absorption spectra of the AuFe18 alloy recorded using a resonant detector at temperatures of 5, 50, and 100 K and respective distribution functions of hyperfine magnetic fields. The solid curves on the left and the distribution functions $P(B_{hf})$ were calculated using the model described in the text.

B_{hf} and the quadrupole shift Δ_Q , its sign being taken into account. Namely, all atomic configurations with larger B_{hf} should have a negative shift Δ_Q , and configurations with a smaller B_{hf} should have a positive Δ_Q . This correlation directly follows from the dependence of B_{hf} and Δ_Q on the orientation of the vector \mathbf{B}_{hf} with respect to the principal axis of the electric-field-gradient tensor. The quadrupole shift of the first and sixth components of the magnetic sextet is

$$\Delta_Q = \frac{e^2 q Q}{4} \frac{3 \cos^2 \theta - 1}{2},$$

where q is the electric-field gradient, Q is the nuclear quadrupole moment, θ is the angle between the principal axis of the electric-field-gradient tensor and \mathbf{B}_{hf} . You can see that Δ_Q varies between $e^2 q Q/4$ ($\theta=0^\circ$) and $-e^2 q Q/8$ ($\theta=90^\circ$). The anisotropic contribution to B_{hf} is also a function of θ and is proportional to $\cos^2 \theta$ in the pseudodipole approximation.¹³ All atomic configurations with nonspherical distributions of the electron density can be classified in two groups: those with the electron-density distribution extended along the axis of the electric-field-gradient tensor (type I with $e^2 q Q < 0$) and those with the electron density compressed along the axis (type II with $e^2 q Q > 0$). Let us take into account that in the model of pseudodipole contribution to \mathbf{B}_{hf} and in accordance with the experimental data, the anisotropic contribution increases B_{hf} if the exchange field is aligned with the larger axis of the ellipsoid of the electron-density distribution. It is obvious that in configurations of type I B_{hf} is maximum at $\theta=0^\circ$, and the quadrupole shift in this case is also maximum and negative. At $\theta=90^\circ$ B_{hf} is minimum and the shift Δ_Q is positive. In the configurations of type II the correlation is opposite (at $\theta=0^\circ$ B_{hf} is minimum and the shift Δ_Q is positive), but in both cases negative shifts Δ_Q correspond to higher B_{hf} and positive Δ_Q to lower B_{hf} . Thus we have derived the permanent correlation between Δ_Q and B_{hf} , which is needed to account for the observed asymmetry of spectra. Since both Δ_Q and the anisotropic contribution to B_{hf} are linear functions of $\cos^2 \theta$, a fairly accurate correlation can be used:

$$\Delta_Q = a + b B_{\text{hf}}, \quad (1)$$

where a and b are constants ($a > 0$, $b < 0$). This model is fairly adequate to account for the shape of the spectrum if the natural assumption about a random distribution of Fe atoms in AuFe disordered alloys holds.

In order to process spectra recorded at 5 K, we used a histogram technique similar to that proposed by Hesse and Rubartsch.¹⁴ The distribution function $P(B_{\text{hf}})$ of the hyperfine field was derived by minimizing the χ^2 functional using the FUMILI computer code. Besides the distribution function, we also varied the relative intensities of the second and fifth components of the magnetic sextets, isomeric shift, and correlation constants in Eq. (1). Our calculations were based on the assumption that the initial resonant lines are described by Lorentzian contours. This assumption is fairly plausible, since we used thin absorbing samples. The resonant absorption in spectra of Fig. 2 was relatively high because we used resonant detectors with a high signal-to-background ratio. In testing calculations we used lines with Gaussian shapes, but

the essential results of our simulations were not affected by this substitution. In order to exclude uncertainties caused by the smoothing procedure in the original technique, the number of intervals of the histogram was selected so that their widths should not be essentially less than the initial-component width. Thus correlations between parameters of the distribution function were minimized and the smoothing procedure was excluded. The width of the interval to satisfy these requirements was selected empirically. Some degradation of the resolution due to the wide histogram components was not essential for our results. The widths of intervals in distribution functions of exchange fields (see below) were selected using similar criteria. The resulting χ^2 varied between 0.9 and 1.5, which indicated the correctness of the processing technique and the reliability of uncertainty estimates for derived parameters.

The major simplification of our model was the assumption that the factors a and b in Eq. (1) were constant for all atomic configurations. This statement is undoubtedly not exact. We performed testing calculations with more complicated models (for example, with two correlation functions like that in Eq. (1) or more complex functions $\Delta_Q(B_{\text{hf}})$). The number of variable parameters did not essentially affect the distribution function $P(B_{\text{hf}})$. In this paper we will only consider results obtained with Eq. (1).

A distribution function of the hyperfine-field distribution in the AuFe18 alloy at $T=5$ K and in zero magnetic field is shown in Fig. 2. At this temperature the distribution functions for both AuFe14 and AuFe18 alloys are practically identical. It is noteworthy that at 5 K the distribution $P(B_{\text{hf}})$ is totally controlled by the anisotropy of the magnetic hyperfine interaction. We assume that at 5 K the magnetic system is in the ground state and all exchange fields are saturated.

The derived relative intensities of magnetic hyperfine spectral components in zero field correspond to random alignments of magnetic moments. The averaged fields $\langle B_{\text{hf}} \rangle$ at $T=5$ K in AuFe14 and AuFe18 alloys were found to be 29.5 ± 0.2 and 30.3 ± 0.2 T, respectively.

3.2. Distribution functions $P(B_{\text{hf}})$ at temperatures above 5 K

AuFe alloys are characterized by wide distributions of exchange fields, which is caused by the random distribution of iron atoms in the lattice and the strong radial dependence of the exchange interaction. The exchange field acting on a given Fe atom is a random value not related directly to the field B_{hf} at this atom in the ground state (at 5 K). Below we assume that in terms of the exchange fields acting on them all Fe atoms are statistically equivalent.

It is obvious that it is incorrect to apply the data processing technique for spectra recorded at 5 K to higher temperatures. In fact, in the interesting temperature range (i.e., in the region of magnetically ordered phases) the quadrupole interaction is constant as a function of temperature to a good approximation. At the same time, B_{hf} drops with temperature, and its decrease is a function of the exchange field acting on a given Fe atom. Thus the technique based on Eq. (1) cannot be used in this case, and at temperatures higher

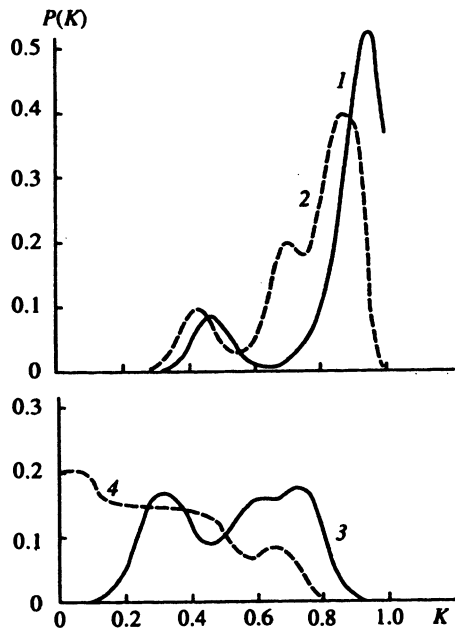


FIG. 3. Distributions of reduced exchange fields $P(K)$ in AuFe14: 1) at 20 K; 2) 30 K; 3) 40 K; 4) 50 K.

than 5 K we employed a modified histogram technique in which the distribution function $P(B_{\text{hf}})$ is calculated in two steps.

The initial function is that derived from spectra recorded at 5 K, $P(B_{\text{hf}}, 5 \text{ K})$. Then for $T > 5 \text{ K}$ each small interval of this function is transformed to a distribution corresponding to a temperature dependence of the reduced exchange field acting on Fe atoms. At $T = 5 \text{ K}$ all reduced fields equal unity. For $T > 5 \text{ K}$ all reduced exchange fields may vary between zero and unity in accordance with the distribution function of the reduced exchange field, $P(K)$, $0 \leq K \leq 1$. Each initial value of B_{hf} is multiplied by $K \leq 1$ and the resulting spectrum is calculated as a superposition of partial spectra corresponding to all intervals of the function $P(K)$ and all intervals of the initial distribution $P(B_{\text{hf}}, 5 \text{ K})$ with weights proportional to the product $P(K)P(B_{\text{hf}}, 5 \text{ K})$. The χ^2 functional is minimized similarly, but in this case the varied parameters are components of the distribution function $P(K)$. In fact the interval $0 \leq K \leq 1$ was divided into ten to twenty small intervals, and the results were weakly affected by their number. After calculating $P(K)$, the distribution function $P(B_{\text{hf}})$ of hyperfine fields at a temperature T was calculated as a convolution of $P(B_{\text{hf}}, 5 \text{ K})$ and $P(K)$. With this procedure we not only exclude the difficulty caused by our inability to use a correlation like Eq. (1) at temperatures above 5 K, but also obtained information about the temperature dependence of the exchange-field distribution function. Average values $\langle B_{\text{hf}} \rangle$ were derived as usual from the function $P(B_{\text{hf}}, T)$. Some calculations of $P(K)$ are given in Figs. 3 and 4. Figure 5 shows the averaged hyperfine field versus temperature.

3.3. Measurements in external magnetic field

Measurements in external magnetic field were undertaken to determine the polarization degree of atomic mag-

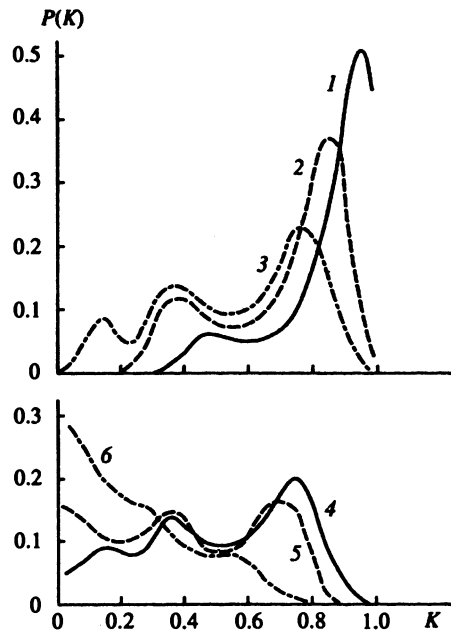


FIG. 4. Distributions of reduced exchange fields $P(K)$ in AuFe18: 1) at 30 K; 2) 50 K; 3) 80 K; 4) 100 K; 5) 110 K; 6) 140 K.

netic moments versus the iron content, external magnetic field, and temperature. The magnetization along an external magnetic field is derived from the relative intensities of the second and fifth components of the sextet in the Mössbauer spectrum. In a general case the intensities of the six components are distributed in the proportion $3:\alpha:1:1:\alpha:3$. In the case of random orientations of moments $\alpha = 2$. This parameter changes with the polarization degree from $\alpha = 2$ to $\alpha = 0$ (in case of saturated polarization in a longitudinal magnetic field) or from $\alpha = 2$ to $\alpha = 4$ (at saturated polarization in a transverse magnetic field).

Measurements of α may be interpreted in two ways. If we assume that a noncollinear magnetic structure is formed in which the moments are aligned primarily with the external magnetic field is formed, the average angle between magnetic moments and the external field may be determined. On the other hand, we may assume that a fraction of atomic

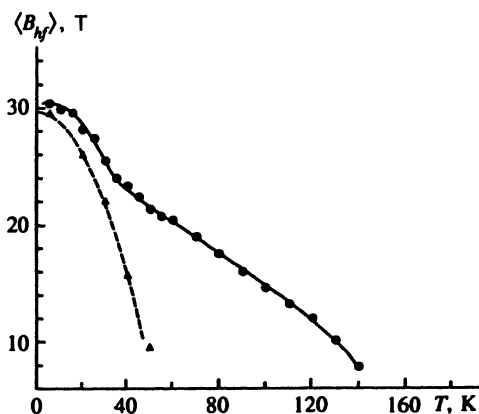


FIG. 5. Averaged hyperfine fields versus temperature in AuFe18 (circles) and AuFe14 (triangles).

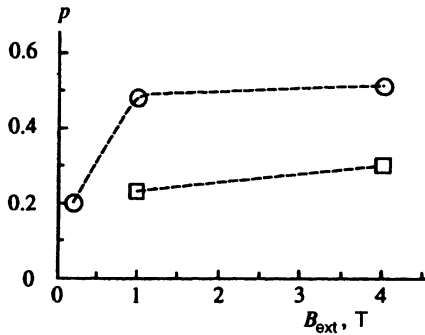


FIG. 6. Polarization degree of Fe atoms versus external magnetic field at $T=5$ K in AuFe18 (circles) and AuFe14 (squares). The dashed lines are guides for the eye.

magnetic moments is totally polarized by the magnetic field and the rest are oriented randomly. In this case the fraction of Fe atoms aligned with the magnetic field can be determined. These two interpretations are equivalent from the formal viewpoint and experimentally indistinguishable. Measurements plotted in Figs. 6 and 7 were interpreted in terms of the second approach. Figure 6 shows the polarization degree of magnetic moments at 5 K in magnetic fields of 0.2, 1.2, and 4.0 T. A large polarization degree of about 50% in AuFe18 is obtained in a field of only 1 T, and at 4 T it is nearly the same. In AuFe14 the polarization degree at 1 T is about twice as low (about 25%) and rises to 30% at 4 T. An interesting result has been obtained in measuring the polarization degree in AuFe18 versus temperature in a weak transverse field of 0.2 T (Fig. 7). At 5 K the polarization is relatively small (about 20%), but it rises rapidly with temperature to 40–50% at $T=35$ K. At higher temperatures the polarization is practically constant.

IV. DISCUSSION

The spin-glass magnetic ordering takes place in AuFe alloys at a very low iron concentration, when the direct exchange interaction between iron atoms is negligible. These alloys are called conventional spin glasses, in which the magnetic ordering at low temperatures is due to the indefinite forms of the indirect exchange interaction acting over a long range. In concentrated AuFe alloys the magnetic ordering at different concentrations and temperatures is controlled by the competition between the long-range indefinite (spin-glass)

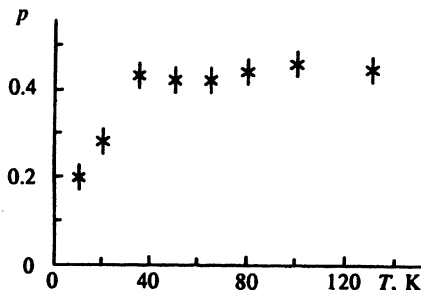


FIG. 7. Polarization of Fe atoms in AuFe18 versus temperature under a magnetic field of 0.2 T.

exchange interaction and the direct exchange interaction between neighboring Fe atoms, which leads to a ferromagnetic ordering.¹⁵ If iron atoms are distributed randomly, local fluctuations of the exchange interaction should be large, and its sign and absolute value should be determined by the local Fe concentration. In regions with a high Fe concentration the direct ferromagnetic Fe–Fe exchange dominates. This should lead to formation of clusters of iron atoms with the predominantly ferromagnetic ordering of spins, whereas in regions with a low local iron concentration the magnetic structure should be that of a spin glass. In alloys with $x < 0.15$ ferromagnetic clusters are largely insulated from each other by regions with a low iron concentration, and orientations of magnetic moments of separate clusters are random, which conforms to a concentrated spin glass. The percolation transition at $x \approx 0.155$ signifies that dimensions of ferromagnetic clusters are sufficiently large that interaction among the clusters is more efficient, large (“infinite”) clusters with the ferromagnetic ordering are formed.

In the range of reentrant spin glasses the competition between the two types of magnetic ordering is most evident. The temperature T_f of the transition to the spin-glass state is considerably lower than the temperature T_C of the transition from ferromagnetic to paramagnetic state. This means that the energy of the indefinite indirect exchange is lower than that of the direct ferromagnetic Fe–Fe exchange. At lower temperatures, when all the exchange fields are nearly saturated, the indefinite exchange prevents formation of large ferromagnetic clusters, which leads to a dominance of the random magnetic structure in the spin-glass phase. The indefinite exchange fields decrease rapidly with the temperature, whereas the fields of the direct Fe–Fe exchange drop more slowly. The decrease in the indefinite exchange field favors integration of small ferromagnetic clusters in large clusters that leads to the transition to the ferromagnetic state at T_f . In AuFe18 alloy this transition takes place in a temperature range of 30–50 K. In alloys with the Fe concentration lower than the percolation threshold, small ferromagnetic clusters remain insulated even at higher temperatures, and the transition to the paramagnetic states occurs before the conditions are favorable for the formation of large ferromagnetic clusters.

Measurements of the two alloys with the iron concentration below and above the critical value ($x=0.14$ and $x=0.18$) confirm the qualitative description of magnetic phases existing at various iron concentration and temperature. The technique of data processing used in our work yielded data about exchange fields acting on Fe atoms versus temperature. These data contain more direct information about the magnetic structure than those derived from the distribution of hyperfine fields, since the latter are secondary with respect to the exchange fields.

Our calculations, some of which are given in Figs. 3 and 4, indicate that the exchange interaction is highly nonuniform. In systems with a relatively uniform distribution of exchange fields, one should have expected a gradual shift of the $P(K)$ maximum and an increase in the width of the distribution function as the temperature approaches the magnetic transition. The real patterns are quite different. At rela-

tively low temperatures (below 20–30 K), in addition to the main distribution peak there are satellite peaks due to the much weaker exchange field at some Fe atoms. These satellites persist over a fairly wide temperature range, which indicates the existence of groups of atoms acted upon by exchange fields of essentially different intensities. Given that the direct ferromagnetic exchange energy is considerably larger than the spin-glass exchange energy, it is natural to suggest that the main peak of the distribution function $P(K)$ at maximum K is due to regions with a higher local iron concentration and a predominantly ferromagnetic ordering (“ferromagnetic clusters”). The satellite peaks should correspond to Fe atoms in regions with lower iron concentrations, where the weaker indefinite exchange interaction dominates. These regions may be located in gaps between ferromagnetic clusters and also on cluster boundaries.

An important point is that the main maxima of the distribution functions are clearly defined even at temperatures close to that of the magnetic transition. In AuFe14 three maxima whose positions versus temperature are described by different functions are observed at temperatures of 30 and 40 K. The shape of the distribution function changes rapidly in a range of 40–50 K. At 50 K a local maximum is seen around $K=0$, which corresponds to a transition of a fraction of Fe atoms to the paramagnetic state (“spin melting”¹¹). In AuFe18 the structure with three peaks persists at temperatures of up to ≈ 100 K. At higher temperatures the probability of zero or very low exchange fields grows rapidly. This indicates that a fraction of Fe atoms in regions with a low iron concentration transfer to the paramagnetic (or almost paramagnetic) state at a temperature 20–50 K lower than the Curie point. Note that on the initial stage of “spin melting” the intensity of the maximum around zero exchange field approximately corresponds to the fraction of Fe atoms which do not have other Fe atoms among their nearest neighbors.

The positions of maxima of the distribution function $P(K)$ versus temperature can be interpreted in terms of the generalized mean-field approximation. For AuFe alloys this model is certainly very approximate, however, it allows a semiquantitative interpretation of the shape of the $P(K)$ curve and a clear explanation of the nature of satellite peaks. The position of the main maximum as a function of temperature is well approximated by the Brillouin function

$$m_1(T) = B_S \left(\frac{3S}{S+1} \frac{mT_C}{T} \right), \quad (2)$$

where S is the effective spin and m is the reduced local magnetization. As for the satellite peaks, we must take into account that the exchange field is weaker than for the case of the main peak. In a general case (in terms of the generalized mean-field approximation) the satellite-peak position versus temperature can be expressed as

$$m_{II}(T) = f B_{S'} \left(\frac{3S'}{S'+1} \frac{mT_C}{T} R \right) + (1-f)m_1(T), \quad (3)$$

where S' is the effective spin of a group of atoms in a region with a lower exchange field, R is the reduction factor of the exchange field, and f is the factor taking into account relative contributions of the local exchange interaction for a

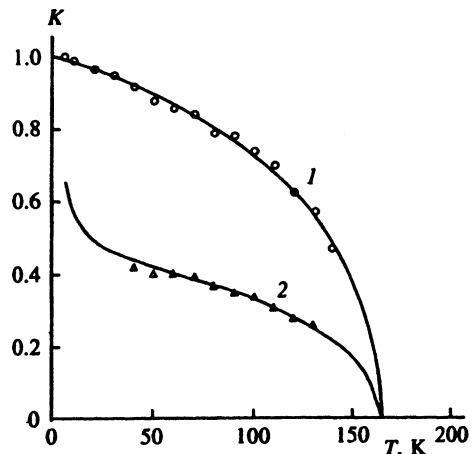


FIG. 8. Positions of the main peak (circles) and the first satellite peak (triangles) in the distribution of the reduced exchange field as a function of temperature in AuFe18. Curve 1 was calculated by Eq. (2) with parameters $S=30$, $T_C=164$ K; curve 2 was calculated by Eq. (3) with parameters $R=0.02$, $f=0.56$.

given group of atoms and the mean exchange interaction corresponding to the Curie temperature. Figure 8 shows some calculations by this model for AuFe18. You can see that the mean-field approximation well describes the positions of the main and satellite peaks versus temperature. The agreement between calculations and experimental data is good at a large effective spin ($S > 20$), which is consistent with the accepted model of the alloy magnetic structure, in which the main peak corresponds to a large group of atoms with ferromagnetic ordering. The Curie temperature for AuFe18 and the temperature of the transition to the spin-glass phase in AuFe14 were determined at 164 ± 2 and 63 ± 2 K, respectively.

Note that the kink on the curve of the mean hyperfine field versus temperature for AuFe18 (Fig. 5) is evidently due to the emergence of the satellite peaks in the distribution $P(K)$. This kink is only indirectly related to the transition from the spin-glass to ferromagnetic state, and it should not be interpreted in terms of freezing of transverse magnetic moment components, as is suggested, for example, by the model proposed by Gabay and Toulouse.⁹

The proposed model of the magnetic structures of AuFe alloys is consistent with measurements of the local Fe magnetization in an external magnetic field (Figs. 6 and 7). A considerable local magnetization was measured under strong magnetic fields at 5 K in both AuFe18 and AuFe14 in the spin-glass state. The polarization degree in AuFe18, however, is about twice as large (about 50%, Fig. 6). A similar result was obtained in an alloy with $x=0.168$ in a field of 2 T.¹⁶ It is natural to suggest that this high polarization in the spin-glass phase is due to the polarization of clusters with predominantly ferromagnetic ordering of Fe moments. The strength of interaction of such clusters with an external magnetic field may be fairly high, and in a field of only 1 T the spin-glass structure of an alloy can be effectively destroyed by the alignment of Fe spins with the external magnetic field. In AuFe14 this effect is considerably weaker, but in a field of 4 T the polarization is also notable (about 30%). After the

transition across the percolation threshold, the polarization of the spins is considerably higher, but our results indicate that there are groups of atoms with predominantly ferromagnetic spin alignment even in AuFe14.

Measurements of the AuFe18 polarization degree versus temperature in a weak magnetic field of 0.2 T are very interesting (Fig. 7). Even in such a low field, a notable polarization of about 20% could be detected at 5 K. The polarization rapidly increases with temperature to 40–45% at $T > 35$ K. Note that this value is close to that measured in this alloy at 5 K in strong magnetic fields. This result may be interpreted as an evidence in favor of the spin transition predicted by Saslow and Parker¹¹ for systems with competing exchange interaction. In the idealized model¹¹ this transition takes place in a very narrow temperature range. In a real AuFe alloy its width is 10–20 K. Note that the polarization in AuFe18 in a strong magnetic field at 5 K or in a weak magnetic field at a temperature higher than 35 K is close to the integrated intensity of the main peak of $P(K)$. In AuFe14 in a weak magnetic field only a small polarization of the magnetic moments was detected, which corresponds to the spin-glass state at an iron concentration below the percolation threshold.

The proposed model is in a qualitative agreement with measurements of neutron depolarization in $Au_{1-x}Fe_x$ ($x=0.16$ and 0.19) versus temperature and magnetic field.¹⁷ Those measurements indicate that in alloys with an iron concentration below the percolation threshold, the predominantly ferromagnetic alignment of magnetic moments in large clusters persists when samples are cooled in a magnetic field to a temperature below that of the phase transition to spin glass.

V. CONCLUSIONS

Measurements of the hyperfine structure of Mössbauer spectra of $Au_{1-x}Fe_x$ ($x=0.14$ and 0.18) at different temperatures and fields have been interpreted in terms of a new model which accounts for the shapes of spectra at 5 K and allows us to calculate not only the distributions of the hyperfine field, but also the distributions of the exchange fields acting on Fe atoms at different temperatures. A model of the magnetic structure of AuFe alloys with iron concentrations

below and above the percolation threshold has been suggested. The magnetic structure and mode of magnetic ordering are determined by the competition between the indefinite exchange long-range interaction shaping the spin-glass phase and the stronger short-range ferromagnetic interaction among Fe atoms. The magnetic structure of alloys at different iron concentrations and temperatures has been interpreted in terms of Fe clusters with predominantly ferromagnetic ordering in regions with a high iron concentration and prevalence of the weaker, indefinite (spin-glass) exchange interaction in regions with a lower iron content. Satellite peaks in distributions of exchange fields reflect local fluctuations of the magnitude and sign of the exchange interaction. The proposed model is justified by measurements of Fe polarization in weak and strong magnetic fields at different temperatures. A strong temperature dependence of the local magnetization has been detected in AuFe18 in a weak magnetic field of 0.2 T, which may be interpreted as a transition predicted by Saslow and Parker.¹¹

¹B. H. Verbeek and J. A. Mydosh, *J. Phys. F* **8**, L109 (1978).

²W. Abdul-Razzaq, J. S. Kouvel, and H. Claus, *Phys. Rev. B* **30**, 6480 (1984).

³R. A. Brand, J. Lauer, and W. Keune, *Phys. Rev. B* **31**, 1630 (1985).

⁴M. M. Abd-Elmeguid, H. Micklitz, R. A. Brand, and W. Keune, *Phys. Rev. B* **33**, 7833 (1986).

⁵S. Lange, M. M. Abd-Elmeguid, and H. Micklitz, *Phys. Rev. B* **41**, 6907 (1990).

⁶C. Meyer and F. Hartmann-Boutron, *Hyperf. Inter.* **59**, 219 (1990).

⁷A. L. Erzinkyan, V. P. Parfenova, S. I. Reyman *et al.*, *Hyperf. Inter.* **78**, 491 (1993).

⁸G. M. Gurevich, S. V. Topalov, A. L. Erzinkyan *et al.*, *Hyperf. Inter.* **78**, 497 (1993).

⁹M. Gabay and G. Toulouse, *Phys. Rev. Lett.* **47**, 201 (1981).

¹⁰P. A. Beck, *Phys. Rev. B* **32**, 7255 (1985).

¹¹W. M. Saslow and G. Parker, *Phys. Rev. Lett.* **56**, 1074 (1986).

¹²Y. Yoshida, F. Langmayr, P. Fratzi, and G. Vogl, *Phys. Rev. B* **39**, 6395 (1989).

¹³N. N. Delyagin, V. I. Nesterov, and A. K. Churakov, *Zh. Éksp. Teor. Fiz.* **93**, 1480 (1987) [*Sov. Phys. JETP* **66**, 844 (1987)].

¹⁴J. Hesse and A. Rubartsch, *J. Phys. F* **7**, 526 (1974).

¹⁵J. J. Smit, C. J. Nieuwenhuys, and L. J. de Jongh, *Sol. St. Commun.* **32**, 233 (1979).

¹⁶J. Lauer and W. Keune, *Phys. Rev. Lett.* **48**, 1850 (1982).

¹⁷S. Mitsuda, H. Yoshizawa, T. Watanabe *et al.*, *J. Phys. Soc. Jap.* **60**, 1721 (1991).

Translation provided by the Russian Editorial office.